LATE CARBONIFEROUS WOODY DEBRIS, SECONDARILY EMBEDDED IN QUATERNARY DEPOSITS IN THE SUDETY MTS., SW POLAND

Adrianna MAĆKO[1]*, Aleksander KOWALSKI[1] & Ronny ROESSLER[2, 3]

[1] *Polish Geological Institute - National Research Institute, Lower Silesian Branch of Henryk Teisseyre in Wrocław, Jaworowa 19, 50-122 Wrocław, Poland;*
e-mails: adrianna.macko@pgi.gov.pl, aleksander.kowalski@pgi.gov.pl
[2] *Museum für Naturkunde Chemnitz, Moritzstraße 20, 09-111 Chemnitz, Germany*
[3] *Technical University Bergakademie Freiberg, Geological Institute, Bernhard-von-Cotta-Straße 2, 09599 Freiberg, Germany ; e-mail: roessler@naturkunde-chemnitz.de*
**Corresponding author*

Maćko, A., Kowalski, A. & Roessler, R., 2026. Late Carboniferous woody debris, secondarily embedded in Quaternary deposits in the Sudety Mts., SW Poland. *Annales Societatis Geologorum Poloniae,* 96: xx–xx.

Abstract: Several dozen samples of silicified wood were discovered during a renewed geological mapping survey in the Sudetes Mountains (NE Bohemian Massif, SW Poland). The material originates from the Metuje River valley, near Kudowa-Zdrój (Kudowa-Słone locality), where woody debris is embedded in the unconsolidated gravelly Quaternary alluvial deposits that form a river terrace. The silicified wood occurs as clasts in a gravelly lithofacies. To determine the taxonomic affinity, taphonomic history, and provenance of the material, the specimens were analysed macroscopically and using petrographic microscopy, cathodoluminescence imaging and scanning electron microscopy. The wood is assigned to *Cordaixylon*, a cordaitalean genus, characteristic of Late Palaeozoic forest ecosystems. Despite its occurrence as barkless and branchless fragments in unconsolidated, Quaternary sediments, the secondary xylem anatomy is exceptionally well-preserved. This combination of anatomical fidelity and physical abrasion indicates that the material is allochthonous and records a multi-stage depositional history. Sedimentological and palaeobotanical evidence demonstrates that the wood was derived from Carboniferous strata and had experienced at least two phases of fluvial redeposition: first within Carboniferous arkosic channel deposits, and later within Late Quaternary river-terrace sediments. Palaeoflow indicators and clast petrography from the Kudowa-Słone exposure show persistent southward transport of gravel and woody debris, with the principal source area located to the north. These data support a provenance from the Late Carboniferous Jivka Member of the Odolov Formation, in the eastern (Czech) part of the Intra-Sudetic Basin, where cordaitalean wood is abundant and exposed in Carboniferous strata, incised by the Metuje and Dřevič rivers.

Key words: Silicified wood, fossil redeposition, facies analysis, palaeocurrent analysis, Intra-Sudetic Basin, Krkonoše Piedmont Basin.

Manuscript received 22 December 2025, accepted 16 April 2026

INTRODUCTION

Silicified wood is a common element of sedimentary successions, preserved in Late Palaeozoic basins across Central Europe, particularly those formed during or after the Variscan orogeny (Trümper *et al.*, 2018). The wood remains are typically associated with Carboniferous and Early Permian siliciclastic deposits and occur in a wide range of sedimentary environments, from coal-bearing swamp successions to complex fluvio-lacustrine systems (Trümper *et al.*, 2018). Well-documented occurrences of fossil wood have been described from the Saar-Nahe Basin in Germany (Trümper *et al.*, 2018; Rößler *et al.*, 2021), the Saale Basin (Trümper *et al.*, 2020), the Pilsen-Trutnov Basin Complex in the Czech Republic and Poland (Opluštil *et al.*, 2024), as well as the Donets Basin in Ukraine (Trümper *et al.*, 2022). Despite differences in basin evolution and tectonic setting, a common feature across these regions is the preservation of fossil wood through silicification, a process that captures anatomical features, and provides valuable insights into past vegetation and depositional environments (Akahane *et al.*, 2004; Mustoe, 2015, 2023; Rößler *et al.*, 2021; Trümper *et*

al., 2022). The plant fossil-rich sediments accumulated during a time of significant Late Palaeozoic climatic and tectonic transformation, coinciding with the assembly of the supercontinent Pangea and the final stages of the Variscan Orogeny (Schneider *et al.*, 2020). During the Late Carboniferous, present-day Central Europe was situated near the palaeoequator and experienced a warm, humid climate that supported the development of extensive coal-forming wetlands and dense, diverse forest ecosystems (Cleal and Thomas, 2005; DiMichele, 2014). The Variscan mountain belt, formed through the collision of Gondwana and Laurussia, was subsequently fragmented into a mosaic of sedimentary basins (Schneider *et al.*, 2020). These basins and their surrounding areas preserve a valuable geological archive of tectonic activity, climatic oscillations, erosion of uplifted source regions, and the widespread expansion of vegetation across the equatorial zone of the supercontinent Pangea (DiMichele, 2014).

In the Sudety Mountains (SW Poland), silicified wood has also been documented, primarily in association with Carboniferous and Permian deposits in the Intra-Sudetic and North-Sudetic basins (Dziedzic, 1959; Nemec, 1984; Mastalerz, 1996; Kurowski, 1998; Madej, 2023). During the Late Carboniferous, the region experienced a warm and humid climate that supported the development of extensive swamp forests within fluvial systems of fault-bounded basins and grabens (Nemec, 1984; Mastalerz, 1990; Opluštil and Pesek, 1998; Nowak and Górecka-Nowak, 1999; Mencl and Sakala, 2009; Opluštil *et al.*, 2016). The most significant occurrences of fossil wood from this period in Poland have been reported in the Wałbrzych and Nowa Ruda areas, located in the northern and eastern parts of the Intra-Sudetic Basin (ISB; Dziedzic, 1959; Brzyski, 1969, 2001; Florjan, 2012). In this area, fossil wood is most commonly associated with coal seams, with well-preserved fragments found in nearby fluvial deposits, where they were transported and incorporated into channel and overbank sediments (Nemec, 1984; Mastalerz, 1996; Kurowski, 1998). The material includes both coalified and silicified specimens. In the latter, silica replaced the original organic tissue, preserving internal anatomical structures instead of allowing complete carbonization. Many of the finds were uncovered during the region's long history of coal mining in Lower Silesia, Poland, which frequently exposed new material during excavation (Dziedzic, 1959; Nemec, 1984).

In contrast to the relatively well-documented occurrences of petrified wood in European post-Variscan basins, the present study focuses on a less frequently described phenomenon – trunk fragments that have been transported and ultimately embedded within Quaternary alluvial sediments. These remains, preserved initially in Late Carboniferous strata of the south-western ISB, were eroded and carried southward by the Metuje River (Czech Republic) and its tributaries. A detailed sedimentological study of Quaternary deposits, exposed near Kudowa-Zdrój, enabled the interpretation of transport pathways and depositional processes, responsible for the accumulation of the fossil wood. As a result, the silicified fragments were found to have been transported from their primary source area and redeposited. Although reworked to varying degrees and incorporated as gravel-sized clasts, the specimens retain fine anatomical detail, offering valuable insights into both the structure of Late Carboniferous forest ecosystems and the Quaternary fluvial processes, responsible for their redistribution. Their occurrence within river terrace sediments highlights the role of post-depositional transport in shaping the fossil record and demonstrates the long-term preservation potential of silicified wood outside of its original stratigraphic context.

GEOLOGICAL SETTING

The fossilized wood fragments were collected from an artificial exposure of unconsolidated Quaternary deposits in Kudowa-Słone, near Kudowa-Zdrój, in SW Poland (Figs 1, 2). The study site is situated on a Metuje River terrace, approximately 13–19 m above the present river level, with the river flowing at approximately 347 m a.s.l., and the exposure scarp reaching 360–370 m a.s.l. Slightly below the studied exposure, at elevations of 355–361 m a.s.l., lie the excavations of abandoned gravel pits that formerly exploited deposits of the lower terrace. Just west of this site, the Klikawa Stream (also known as Bystra) joins the Metuje, which in this sector follows the Polish-Czech border (Fig. 1B). The Metuje River, a 78-km-long left tributary of the Elbe, in its upper course drains the Broumovská vrchovina in the Czech Republic, capturing the middle and marginal parts of the ISB (Fig. 1A) before continuing southwestward toward the Elbe River system. One of the major tributaries of the Metuje that drains the southwestern part of the ISB is

Fig. 1. Geological setting and location of the study area. **A.** Simplified geological map of the study area and adjacent tectonic units, with emphasis on the Intra-Sudetic Basin (ISB). The map is draped over a shaded digital elevation model (DEM), generated from Shuttle Radar Topography Mission (SRTM) data (Farr *et al*., 2007). Abbreviations: BU – Bardo Unit, CzG – Czerwieńczyce Graben, GSM – Góry Sowie Massif, KGP – Karkonosze Granite Pluton, KMC – Kaczawa Metamorphic Complex, KłMC – Kłodzko Metamorphic Complex, K-OGM – Kudowa-Olešnice Granitoid Massif; NMMU – Nové Město Metamorphic Unit, NRM – Nowa Ruda Ophiolite Massif, N-SB – North-Sudetic Basin, OMC – Orlica Metamorphic Complex, RJC – Rudawy Janowickie Metamorphic Complex, S-SGM – Strzegom-Sobótka Granitoid Massif, ŚA – Ścinawka Anticline, ŚwG – Święcko Graben, ŚU – Świebodzice Unit, WoS – Wolibórz Syncline. Faults and fault zones: D-GF – Duszniki-Gorzanów Fault, HPFZ – Hronov-Poříčí Fault Zone, K-ŚF – Krajanów-Ścinawka Fault. Geological map based on Sawicki (1995), modified and supplemented by the authors. The yellow dashed polygon marks the presumed source area of the woody debris in the southwestern part of the ISB, with the inferred direction of its transport (yellow arrow). **B**. Detailed geological map of the study area, superimposed on a shaded 1×1 m LiDAR digital elevation model (after Kowalski *et al*., 2024a). The location of the study site is indicated. The extent of unconsolidated Quaternary deposits is shown, courtesy of Bogusław Przybylski (PGI-NRI).

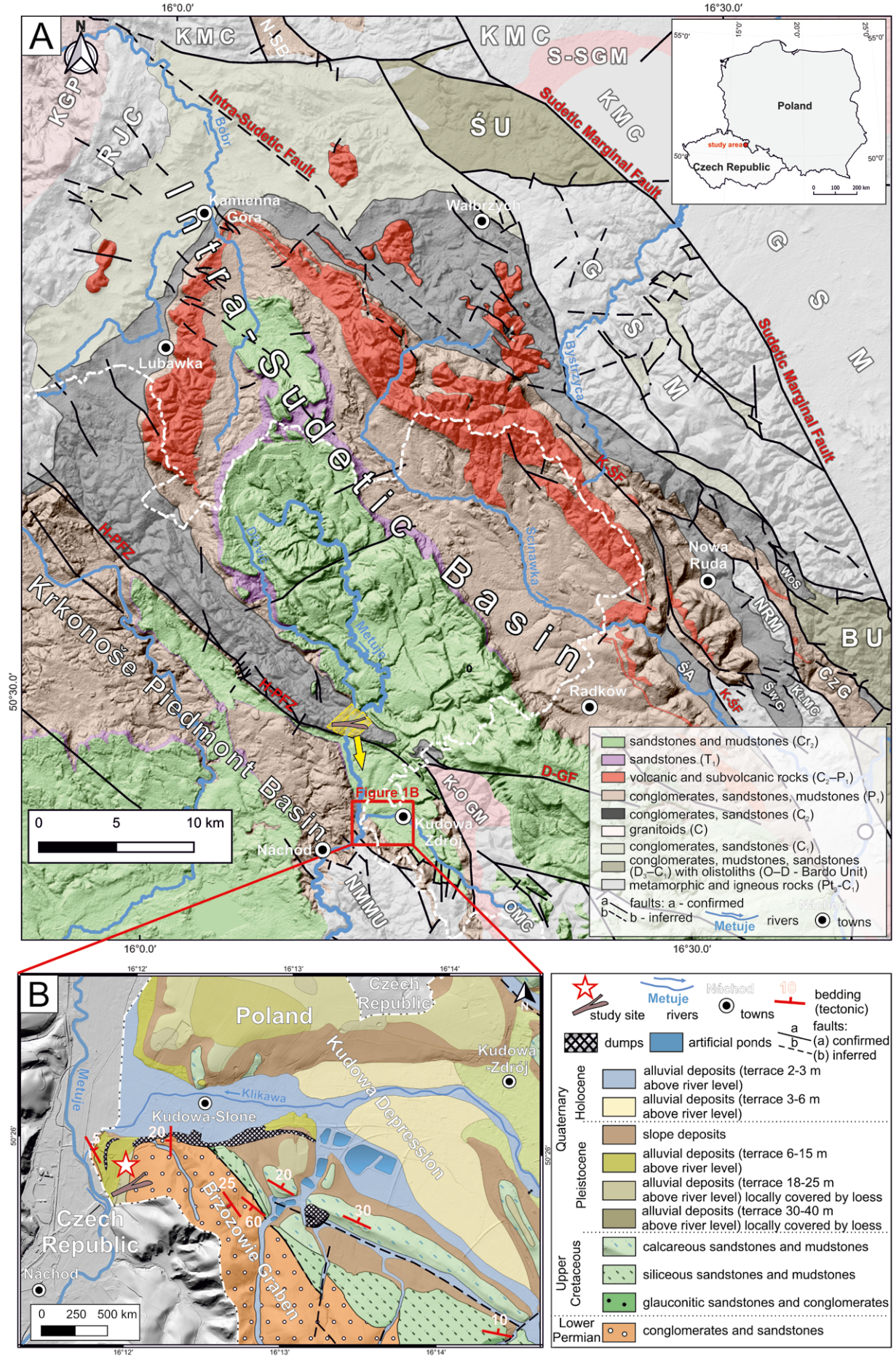
A
B
KMC
S-SGM
ŚU
GSM
BU
RJC
KGP
NSB
SA
SWG
CZG
KMG
NRM
WOS
OMG
NMMU
Intra-Sudetic Basin
Krkonoše Piedmont Basin
Intra-Sudetic Fault
Sudetic Marginal Fault
H-PFZ
K-SF
D-GF
K-O GM
Bóbr
Bystrzyca
Metuje
Dzika
Ścinawka
Kamienna Góra
Wałbrzych
Lubawka
Nowa Ruda
Radków
Náchod
Kudowa Zdrój
Figure 1B
Poland
Czech Republic
study area
0 100 200 km
0 5 10 km
sandstones and mudstones (Cr2)
sandstones (T1)
volcanic and subvolcanic rocks (C2–P1)
conglomerates, sandstones, mudstones (P1)
conglomerates, sandstones (C2)
granitoids (C)
conglomerates, sandstones (C1)
conglomerates, mudstones, sandstones (D3–C1) with olistoliths (O–D - Bardo Unit)
metamorphic and igneous rocks (Pt3-C1)
faults: a - confirmed b - inferred
rivers
towns
Kudowa-Słone
Klikawa
Kudowa Depression
Broumovské Stěny Graben
study site
bedding (tectonic)
dumps
artificial ponds
faults: (a) confirmed (b) inferred
Quaternary
Holocene
Pleistocene
alluvial deposits (terrace 2-3 m above river level)
alluvial deposits (terrace 3-6 m above river level)
slope deposits
alluvial deposits (terrace 6-15 m above river level)
alluvial deposits (terrace 18-25 m above river level) locally covered by loess
alluvial deposits (terrace 30-40 m above river level) locally covered by loess
Upper Cretaceous
calcareous sandstones and mudstones
siliceous sandstones and mudstones
glauconitic sandstones and conglomerates
Lower Permian
conglomerates and sandstones

Fig. 1.

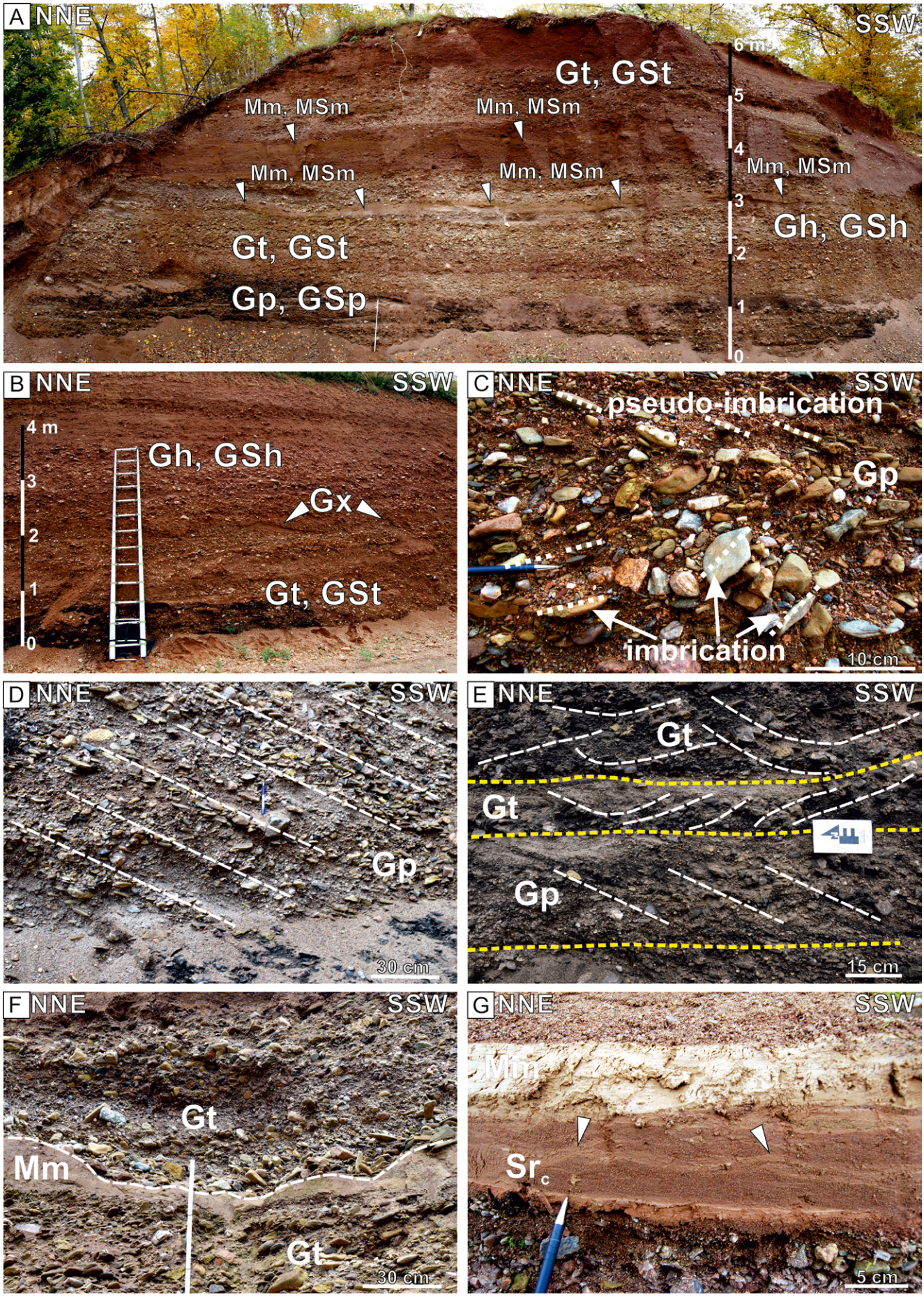
A NNE
SSW
6 m
5
4
3
2
1
0
Gt, GSt
Mm, MSm
Mm, MSm
Mm, MSm
Mm, MSm
Mm, MSm
Gh, GSh
Gt, GSt
Gp, GSp
B NNE
SSW
4 m
3
2
1
0
Gh, GSh
Gx
Gt, GSt
C NNE
SSW
pseudo-imbrication
Gp
imbrication
10 cm
D NNE
SSW
Gp
30 cm
E NNE
SSW
Gt
Gt
Gp
15 cm
F NNE
SSW
Gt
Mm
Gt
30 cm
G NNE
SSW
Mm
Src
5 cm

Fig. 2

the Dřevíč River, a right-bank tributary, about 22 km long, with a catchment area of 46.4 km² (Fig. 1A).

The exact age of the terrace deposits, containing the fossil wood, remains uncertain (Gierwielaniec, 1955). These sediments were originally assigned to the Odranian (Marine Isotope Stage, MIS, 6) Glaciation, with the terrace situated approximately 15 m above the present-day river level, corresponding to the 6–15 m Metuje River terrace level (Cymerman, 2019a, b). However, on the basis of correlations with other fluvial terraces in the Sudetes, it appears more likely that this terrace level corresponds to the higher of the two terraces, formed during the Northern Polish Glaciation – specifically, the Vistulian (MIS 2–4). In line with this interpretation, Przybylski (in Kowalski *et al*., 2024a, b) assigned the studied sediments to alluvium, forming floodplain terraces at 6–15 m and 18–25 m above the present river level, respectively (Fig. 1B).

The floodplain terrace deposits of the Metuje River near Kudowa-Słone rest upon basement rocks, composed of arkosic conglomerates and conglomeratic sandstones of Early Permian age (Fig. 1B; Gierwielaniec, 1955). These strata are exposed in the Brzozowie Graben, a structural outlier of the Krkonoše Piedmont Basin, which forms part of the larger Pilsen-Trutnov Basin Complex (Cháb *et al.*, 2010; Opluštil *et al.*, 2016). The sedimentary succession of the Krkonoše Piedmont Basin attains a total thickness of approximately 1,800 m and comprises non-marine deposits, ranging in age from Late Carboniferous (Moscovian–Kasimovian) to Early Triassic (Pešek *et al*., 2001; Schöpfer *et al.*, 2022). In the Polish part of the basin, however, the Brzozowie Graben is considered part of a larger tectonic unit, known as the Kudowa Depression (Gierwielaniec, 1965; Wojewoda and Burliga, 2008), which is composed of continental Lower Permian deposits, unconformably overlain by Upper Cretaceous marine sediments. Lower Permian conglomerates, belonging to this unit, are exposed in the Metuje riverbed, approximately 50 m west of the studied exposure (Fig. 1B).

The Kudowa Depression, together with the Krkonoše Piedmont Basin, is bounded to the northeast by the Hronov-Poříčí Fault Zone, which marks the tectonic boundary with the ISB (Fig. 1A; Wojewoda, 2009; Nováková, 2014; Prouza *et al.*, 2015). The ISB is an NW–SE-oriented intramontane basin of multicyclic origin, extending approximately 70 km in length and 35 km in width across southwestern Poland and the northeastern Czech Republic. Its development began at the end of the Variscan orogeny, during the early to middle Late Viséan (335–333 Ma; Turnau *et al*., 2002), and continued through a prolonged history of discontinuous sedimentation, overprinted by successive deformation phases from the Late Carboniferous to the Late Cretaceous (Augustyniak and Grocholski, 1968; Nemec *et al.*, 1982; Mroczkowski and Mader, 1985; Dziedzic and Teisseyre, 1990; Wojewoda, 1997; Opluštil *et al.*, 2016; Kowalski, 2020, 2021; Głuszyński and Aleksandrowski, 2022). The Palaeozoic part of the basin fill is characterised by a megacyclic architecture that reflects repeated alternations between sedimentation and tectonic subsidence, intermittently interrupted by polymodal volcanic and subvolcanic activity during the Late Carboniferous and Early Permian (Nemec *et al*., 1982; Wojewoda and Mastalerz, 1989; Awdankiewicz, 1999a, b). During this time, fluvial sedimentation predominated in the southwestern ISB, resulting in the deposition of the coal-bearing Žacléř and Glinik formations, the latter being referred to as the Odolov Formation in the Czech part of the basin (Tásler *et al.*, 1979; Mastalerz, 1996; Pešek *et al.*, 2001; Opluštil *et al.*, 2016). The Odolov Formation is further subdivided into the Svatoňovice and Jívka members (Tásler *et al.*, 1979; Opluštil *et al.*, 2016). These arkosic fluvial deposits contain the highest concentration of fossil wood documented in the ISB, mainly in the lower part of the Jívka Member (Matysová *et al.*, 2008; Mencl and Sakala, 2009, Mencl *et al*., 2013; Trümper *et al.*, 2022).

MATERIAL AND METHODS

Silicified wood occurs as clasts in the gravel deposits, preserved as trunks and their fragments, ranging from 5 to 45 cm in length. Most samples were recovered from the scree at the base of the exposure, while seven specimens were documented as embedded in the Quaternary sediments, exposed in the outcrop wall. The specimens lack bark and branches, and most exhibit varying degrees of rounding, indicative of fluvial transport.

The sedimentological study was conducted between 2022 and 2025 at an exposure approximately 100 m long and 4–8 m high, with a scarp orientation of NNW–SSE (Fig. 3). Representative sections of the outcrop were selected to capture the lithological and facies variability of the Quaternary fluvial deposits. Fieldwork focused on documenting the main textures of the coarse-grained sediments and on identifying the dominant depositional processes. The study involved detailed macroscopic observations, lithofacies classification, and systematic vertical logging to record sedimentary structures, grain-size variability, and unit boundaries. Maximum particle sizes (MPS) were measured within individual lithofacies, and facies types were classified according to schemes widely used in fluvial sedimentology (Miall, 1977a, b, 1996), with minor modifications to ensure consistency

Fig. 2. Sedimentological characteristics of Quaternary deposits exposed at the Kudowa-Słone locality. **A**–**B.** Main features and the main distinguished lithofacies within the Quaternary deposits. Note the predominance of gravelly lithofacies, accompanied by a minor proportion of discontinuous lenses of fine-grained deposits, assigned to the Mm and MSm lithofacies (arrowed), as well as gravels with backset cross-stratification and/or sinusoidal cross-stratification (Gx) in the middle part of the exposure (B). **C**. Well-developed clast imbrication [a(t)–b(i) fabric] beneath the Gp unit, additionally showing clast pseudo-imbrication dipping in the direction of the foresets. **D**. Solitary Gp unit in the lower part of the Kudowa-Słone exposure. **E**. Gravelly units of Gp and Gt, bounded by erosional surfaces (yellow dashed lines). **F**. Concave-up scour filled with the Gt lithofacies, incised into fine-grained deposits of the Mm lithofacies. **G**. Fine-grained Sr_c deposits with mud drapes (arrowed), passing upward into massive muds of the Mm lithofacies.

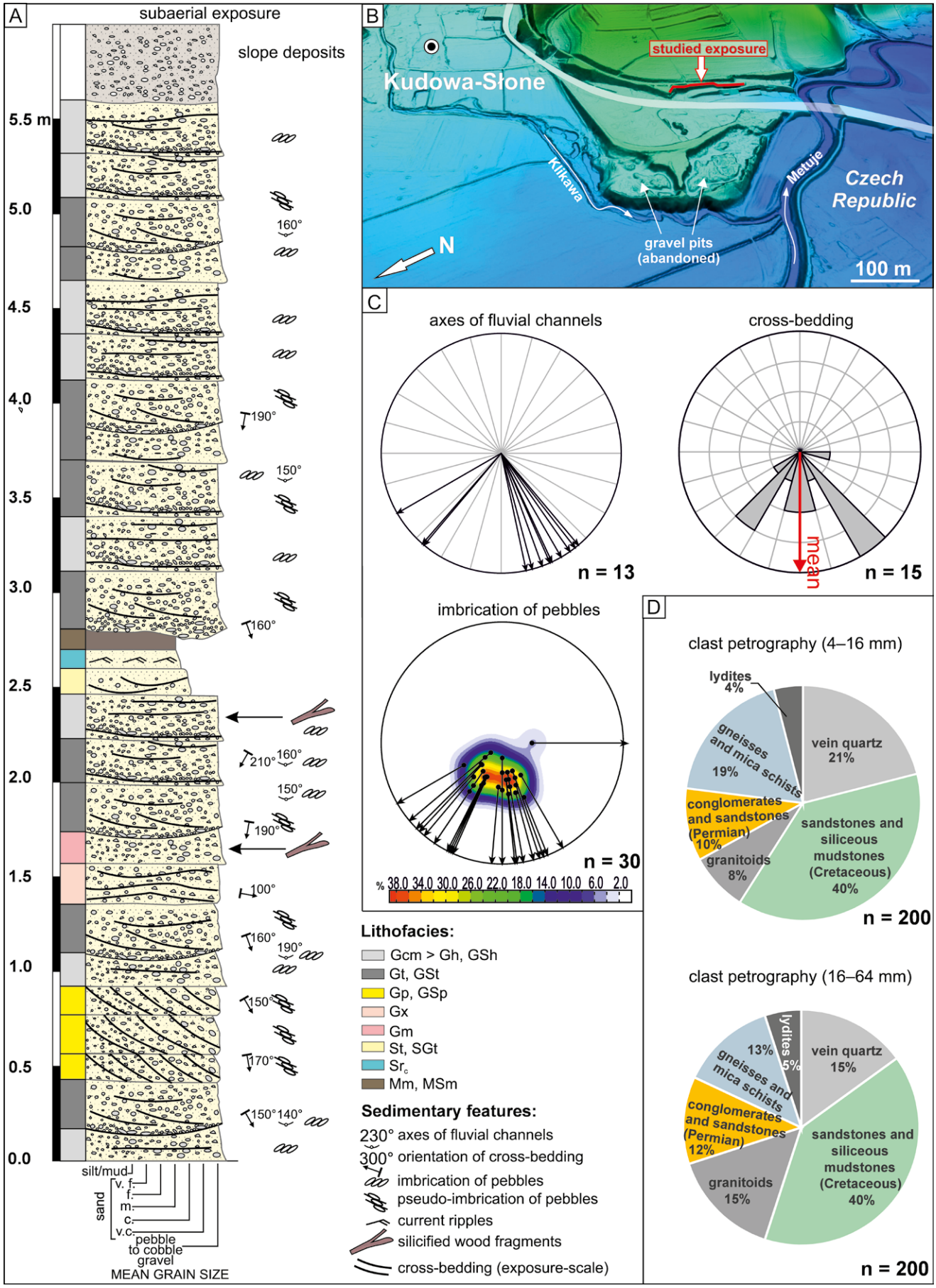
A
subaerial exposure
slope deposits
5.5 m
5.0
4.5
4.0
3.5
3.0
2.5
2.0
1.5
1.0
0.5
0.0
160°
190°
150°
160°
210°
160°
150°
190°
100°
160°
190°
150°
170°
150°
140°
silt/mud
sand
v. f.
f.
m.
c.
v.c.
pebble
to cobble
gravel
MEAN GRAIN SIZE
B
studied exposure
Kudowa-Słone
Kłikawa
Metuje
Czech Republic
N
gravel pits (abandoned)
100 m
C
axes of fluvial channels
n = 13
cross-bedding
mean
n = 15
imbrication of pebbles
n = 30
% 38.0 34.0 30.0 26.0 22.0 18.0 14.0 10.0 6.0 2.0
Lithofacies:
Gcm > Gh, GSh
Gt, GSt
Gp, GSp
Gx
Gm
St, SGt
Sr
Mm, MSm
Sedimentary features:
230° axes of fluvial channels
300° orientation of cross-bedding
imbrication of pebbles
pseudo-imbrication of pebbles
current ripples
silicified wood fragments
cross-bedding (exposure-scale)
D
clast petrography (4–16 mm)
lydites 4%
gneisses and mica schists 19%
vein quartz 21%
conglomerates and sandstones (Permian) 10%
granitoids 8%
sandstones and siliceous mudstones (Cretaceous) 40%
n = 200
clast petrography (16–64 mm)
lydites 5%
13%
gneisses and mica schists
vein quartz 15%
conglomerates and sandstones (Permian) 12%
granitoids 15%
sandstones and siliceous mudstones (Cretaceous) 40%
n = 200

Fig. 3.

across the exposure. Particular emphasis was placed on analyzing the geometry, stacking patterns, and lateral relationships of sedimentary bodies. High-resolution photomosaics and interpretive sketches were prepared for representative parts of the outcrop, thereby enabling the documentation of architectural elements and bounding surfaces at the exposure scale. In addition, palaeocurrent indicators – including cross-bedding orientations, palaeochannel-axis trends, and pebble imbrication – were recorded and visualized using rose diagrams, pole-point plots, and contour diagrams. To infer the provenance of the analyzed deposits, a detailed clast-petrography study was carried out on 200 gravel-sized particles from two granulometric fractions (4–16 mm; 16–64 mm). To characterize the silicified wood from the Kudowa-Słone locality, samples were fractured to expose radial and tangential surfaces, from which polished sections were prepared. Additionally, polished sections and standard thin sections were prepared in transverse, tangential, and radial orientations for microscopic analysis. Anatomical features were examined under a standard petrographic microscope and using cathodoluminescence (CL) and scanning electron microscopy (SEM). Observations in plane-polarized light (PPL) and cross-polarized light (XPL) were carried out with a Zeiss Axioscope 5 microscope, equipped with an Axiocam 208 camera. The images from SEM–BSE were acquired using a Hitachi SU3500 scanning electron microscope, fitted with a Gatan panchromatic CL detector. Analytical conditions included an accelerating voltage of 15 kV, a working distance of 10 mm, a 90% spot size, and a frame-scanning time of 80–160 s.

Cathodoluminescence imaging was performed using a Nikon Eclipse 50i optical microscope, equipped with a CITL CCL mk5-2 CL system and Nikon NIS software. The electron beam was operated at 15 kV and approximately 450 μA, with an exposure time of 6 s. Quantitative measurements of tissue morphology and microscopic features were performed using ImageJ.

RESULTS

Sedimentology and clast petrography

In the Kudowa-Słone exposure, the succession is dominated by gravelly lithofacies (Figs 2, 3A, B), consisting mainly of medium- to coarse-grained (–2 to –8 φ), grey to yellowish gravels. These deposits are primarily clast-supported, with matrix-supported gravels occurring subordinately. The gravelly units locally co-occur with fine- to coarse-grained (2.0 to 0 φ) sands, which form composite beds up to 15–20 cm thick. Fine-grained (sandy and muddy) lithofacies occur sporadically and comprise grey, fine-grained sands, interlaminated with brownish muds and silts (two identified lithofacies), with a total thickness of sets not exceeding 10 cm.

Within the coarse-grained gravelly deposits, nine lithofacies were distinguished (Figs 2, 3). The most common are massive, clast-supported gravels (Gcm), typically occupying the lower parts of beds, with sharp, erosive boundaries and grading upwards into horizontally stratified gravels and sandy gravels (Gh, GSh). The lower parts of these beds frequently exhibit well-developed clast imbrication (a(t)–b(i) fabric; Harms *et al.*, 1975; Brenna *et al.*, 2024), with preferred upstream-dipping clasts, indicating sediment transport toward the S and SW (Figs 2C, 3), and secondarily toward the SE. The horizontally stratified gravels pass into planar-stratified gravels or sandy gravels (Gp, GSp; Figs 2D, E, 3A) and trough cross-stratified gravels and sandy gravels (Gt, GSt; Fig. 2E). Within the cross-stratified sets, clasts commonly display pseudo-imbrication (Fig. 2C). The orientation of these cross-strata indicates palaeoflow directed predominantly toward the S and SE, with subordinate transport toward the SW (Fig. 3A, C). Subordinate massive gravels (Gm), forming entire beds of approximately 15–20 cm in thickness, also occur within the succession (Fig. 3A). Locally, gravels with backset cross-stratification and/or sinusoidal cross-stratification (Gx) are present, typically overlying trough cross-stratified units (Figs 2B, 3A). Throughout the exposure, the orientation of fluvial channel axes indicates an overall sediment-transport direction toward the SE, with a subordinate component toward the SW (Fig. 3C).

In the northern sector of the exposure, the gravelly deposits are overlain by brown, ripple-laminated sands (Sr_c), which in turn pass upward into composite beds up to 15 cm thick, composed of discontinuous laminae of brown silts and muds (Mm and MSm lithofacies; Figs 2G, 3A, C). The laterally most extensive mud lens can be traced for several metres, although its thickness remains limited (Fig. 2A).

Clast petrography reveals a consistent compositional pattern across both analysed grain-size fractions (4–16 mm and 16–64 mm; Fig. 3D). In each fraction, the dominant group comprises yellowish Cretaceous sandstones and siliceous mudstones (38–40%) and vein quartz (15–21%). Clasts of medium-grade metamorphic rocks, including gneisses and mica schists, constitute 13–19%, whereas granitoids account for 8–15%. Permian conglomerates and sandstones represent 10–12%, and lydite clasts form a minor component (4–5%).

Interpretation

The analysed succession records deposition within a high-energy, gravel-dominated fluvial system, characterised by bedload-dominated transport and rapid sediment aggradation (Miall, 1977a, 1996; Teisseyre, 1991; Collinson,

Fig. 3. Lithofacies succession, location, palaeoflow indicators and clast composition of the Kudowa-Słone deposits. **A.** Sedimentological log from the Kudowa-Słone exposure, with lithofacies and other sedimentary features indicated. **B**. Detailed location of the study site, shown on a 3D block diagram, generated from LiDAR data, viewed toward the ESE. **C**. Rose diagrams illustrating the measured orientation of fluvial channels and cross-bedding, with the mean direction of cross-bedding indicated by the red arrow. Point and contour plots show the pebble-imbrication measurements together with the interpreted palaeoflow direction (black arrows). **D**. Percentage composition of gravel clasts (size fractions 4–16 mm and 16–64 mm) shown in pie charts.

1996). The predominance of clast-supported massive gravels (Gcm) in the lower parts of the beds, together with their sharp, erosive basal contacts, indicates repeated episodes of channel scour, followed by relatively rapid infilling of wide channel belts with coarse-grained clastic material. The upward transitions into horizontally and horizontally stratified gravels (Gh, GSh) reflect bedload deposition under upper-flow to transitional lower-flow regimes, corresponding to longitudinal, low-relief bedforms and channel-lag deposits (Miall, 1977a, 1996). Planar-stratified gravels (Gp, GSp) and trough cross-stratified gravels (Gt, GSt) reflect the migration of two- and three-dimensional gravelly bedforms within moderately sinuous channel segments (Harms *et al.*, 1975; Allen, 1982; Bridge, 2003; Miall, 2014). The rare occurrence of backset and sinusoidal cross-stratification in gravelly lithofacies (Gx) points to the development of bedforms, related to upper-flow flow regime conditions and local hydraulic jumps, including cyclic steps, chutes-and-pools, antidunes and humpback dunes, generated during high-magnitude flood events (Bridge, 2003; Fielding, 2006; Lang and Winsemann, 2013; Cartigny *et al*., 2014; Slootman and Cartigny, 2020; Weckwerth *et al.*, 2024). Sporadic, thin fine-grained units, comprising ripple-laminated sands (Sr_c) and discontinuous mud and silt laminae of the Mm and MSm lithofacies, are most likely associated with short-lived abandonment of active channels, deposition on bar-margin or interbar surfaces, or shallow overbank sedimentation during waning-flow stages of flood events (Collinson, 1996). The limited thickness, but locally pronounced lateral extent, of the mud layers may also support their interpretation as deposits formed in low-energy overbank settings (Miall, 1996; Bridge, 2003).

Consistent palaeoflow indicators derived from clast imbrication, dips of cross-strata, and the orientation of fluvial-channel axes reveal stable downstream transport toward the S, with deviations toward the SW and SE, implying a relatively constant regional palaeoslope (Fig. 3C). This pattern corresponds to the present-day flow direction of the Metuje River. The petrographic composition of the analysed deposits further supports these interpretations. Cretaceous sandstones and siliceous mudstones dominate the clast composition (up to ~40%) and were derived from the Upper Cretaceous outcrops of the ISB to the north and the Kudowa Depression to the east (Gierwielaniec, 1965; Fig. 1A). Similarly, the silicified wood clasts are interpreted as originating in the lower part of the Jívka Member (Tásler *et al.*, 1979; Opluštil *et al.*, 2016), the outcrops of which in the southwestern ISB contain the highest concentration of fossil wood (Matysová *et al.*, 2008; Mencl and Sakala, 2009; Trümper *et al.*, 2022). A substantial proportion of pinkish granitoid and vein-quartz clasts indicates sediment supply from the Kudowa-Olešnice Granitoid Massif (Żelaźniewicz, 1977a), which is dissected to the southeast of the study site by the Klikawa Stream, a tributary of the Metuje (Fig. 1A). Clasts of gneisses and mica schists most likely originated in the Orlica Metamorphic Complex (Żelaźniewicz, 1977b; Cymerman, 1997), whereas Permian sandstones and conglomerates were probably sourced in the Brzozowie Graben, which underlies the studied Quaternary deposits (Gierwielaniec, 1965).

Overall, the facies architecture of the analysed deposits reflects deposition within a braided or transitional mixed-load gravel-bed river system (Miall, 1996, 2014), subject to fluctuating discharge and high sediment supply, probably associated with recurrent flood episodes. The fossil wood recovered from the exposure is allochthonous, and these flood events most likely were largely responsible for transporting the fossil material from Carboniferous outcrops, located along the southwestern limb of the ISB (Fig. 4).

Palaeobotany

Division GYMNOSPERMOPHYTA (Sternberg, 1820)
Order CORDAITALES (Sternberg, 1820)
Genus *Cordaixylon* Grand'Eury, 1877
Cordaixylon sp.
Fig. 5E, F

Material: 3 specimens, (10KUD, 13KUD, 17KUD) – all from Kudowa-Słone outcrop (50°25′51.3″N, 16°11′56.2″E), deposited in the Lower Silesian Branch of the Polish Geological Institute - National Research Institute.

Remarks: *Cordaixylon* was a widespread element of Carboniferous and Early Permian forest ecosystems, contributing significantly to the structure and composition of swamp and deltaic vegetation. The genus is primarily represented in the fossil record by silicified trunks and secondary wood, which exhibit well-defined anatomical features typical of cordaites. In particular, *Cordaixylon* is distinguished from other cordaite genera by the specific organization of its vascular system and the characteristic structure of its secondary xylem. These features provide reliable criteria for its recognition in fossil assemblages. The anatomy of the wood shows certain similarities to that of modern conifers. However, in detail, it retains traits that link it more closely with primitive gymnosperms, reflecting its intermediate position in the evolutionary history of seed plants. Owing to these attributes, *Cordaixylon* is considered an essential taxon for understanding both the diversity of cordaites and the development of gymnospermous wood during the Late Palaeozoic (Fig. 5).

Description: Plant tissues are well preserved in the majority of thin sections, allowing for detailed observation of their internal structure in both transverse and longitudinal sections (Fig. 6). In all examined specimens, only the secondary xylem is recognizable, while primary xylem could not be detected. The resin canals are absent in all specimens. In the transverse section, the wood is dominated by tracheids, which constitute the principal water-conducting elements. The lumina are generally rectangular to subrectangular in outline, though their contours are frequently irregular, due to diagenetic modifications. Tangential diameters range from 30 to 80 μm, and radial diameters from 20 to 70 μm. The tracheid walls can be up to 10 μm thick, depending on the state of preservation. The lumina remain fairly uniform across the specimen, with an average of about 200 μm. In radial sections, tracheid pits are visible, although not always clearly preserved. The pits are circular to polygonal, usually arranged in three vertical rows. They may be in alternate or opposite patterns. The pits measure about 10 μm

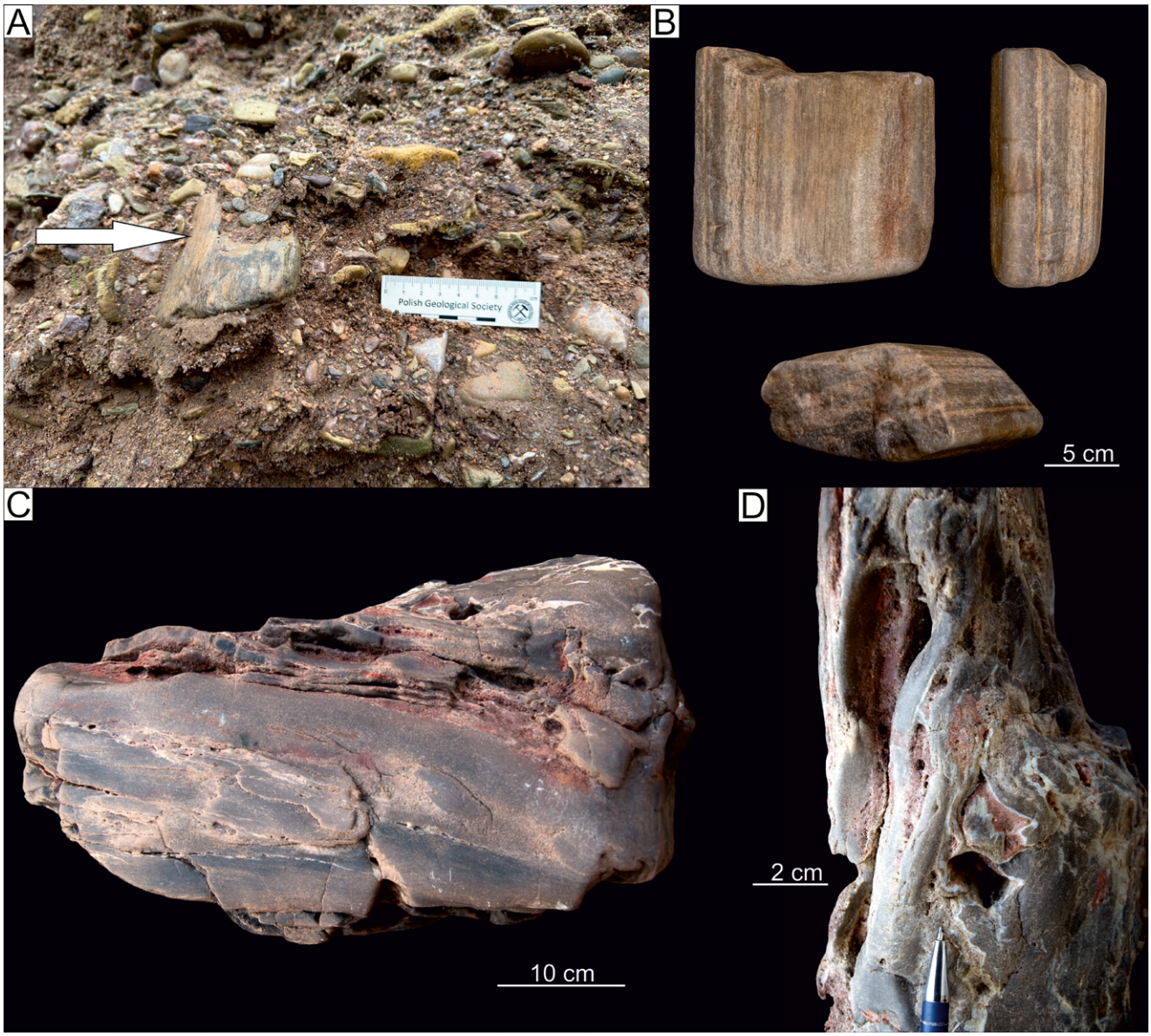

Fig. 4. Macroscopic examples of petrified wood from the Kudowa-Słone exposure. **A**. Fragment of silicified wood, embedded in Quaternary fluvial deposits (arrowed). **B**. Three-dimensional view of the specimen. **C.** The largest sample of silicified wood found at the Kudowa-Słone locality (45 cm along the longest axis). **D.** Close-up view, showing the wood structure.

in diameter (ranging from 6 to 13 µm), with circular apertures about 3 µm wide. Cross-field pits are of the araucarioid type, which is an essential feature for taxonomic interpretation (Fig. 6A). Owing to the silicification, other structural details are not clearly visible.

Discussion: The taxonomic position of Carboniferous gymnosperm wood from the ISB basin requires careful evaluation, in view of earlier classifications. In the past, most anatomically simple secondary woods from these basins were assigned to *Dadoxylon*. However, following the conclusions of Rößler *et al*. (2014), the name *Dadoxylon* is no longer considered valid. Many such woods have subsequently been referred to *Agathoxylon*, a broad collective genus that includes both conifer and cordaitalean forms. The specimens described here, preserve secondary xylem with anatomical features, consistent with cordaitalean wood (Noll, 2012). At the same time, features typical of conifer wood, formerly included in *Dadoxylon* and now commonly placed in *Agathoxylon*, are not observed. On this basis, the material is assigned to *Cordaixylon*, the accepted genus for cordaitalean secondary xylem. Species-level identification is not possible.

Although the specimens assigned to *Cordaixylon* sp. provide well-preserved anatomical detail for reliable generic placement, the exposure also yielded additional silicified wood fragments that could not be identified taxonomically. These remaining specimens do not retain diagnostic microscopic structures. Their internal tissues are partially obscured owing to a combination of factors, mainly later stages of silica recrystallization. Such processes commonly affect redeposited petrified wood and tend to degrade fine cellular features, including pith shape, ray arrangement, and tracheid pit patterns. As a result, these fragments cannot be assigned with confidence, even at the generic level.

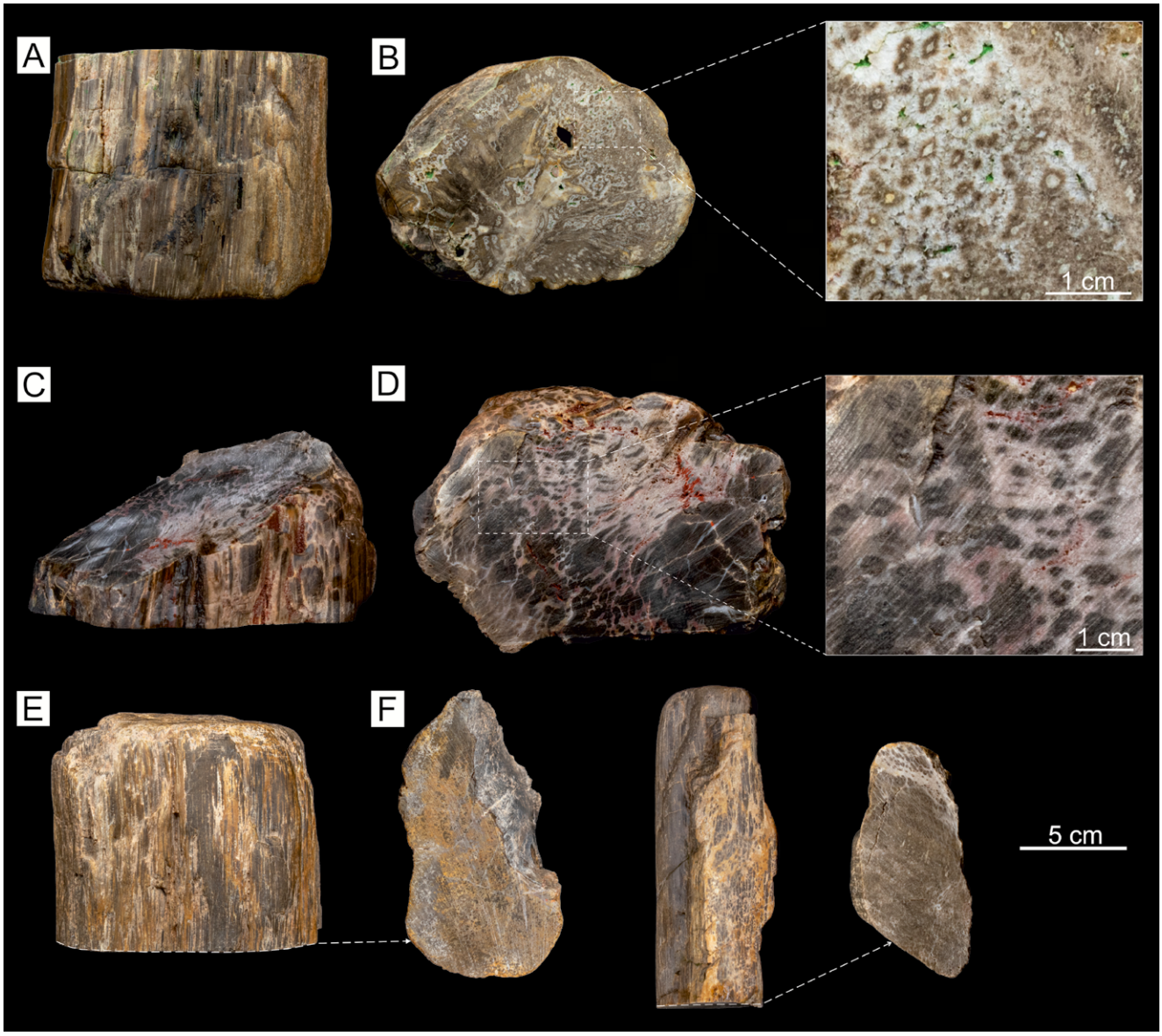

Fig. 5. Macroscopic appearance of selected silicified wood specimens showing variability in preservation style, coloration and internal structures. **A.** Specimen 8KUD – cylindrical trunk fragment with well-preserved longitudinal grain and moderate external weathering. **B.** Transverse view of specimen 8KUD, displaying a cauliflower-like silicification pattern. Inset: cellular-scale preservation with circular to polygonal lumina infilled by silica. **C.** Specimen 5KUD – dark-grey to reddish fragment of the specimen with well-defined wood grain and locally enhanced iron staining. **D.** Transverse view of specimen 5KUD with patchy reddish pigmentation; inset: internal structure showing homogeneously silicified tissue with darker spots corresponding to Fe-rich inclusions. **E.** Specimen 10KUD – a short, cylindrical trunk fragment with well-preserved wood fabric; inset: the exposed fracture reveals compact silicification. **F.** Specimen 17KUD – an elongated piece of silicified wood with an uneven external surface; inset: transverse fracture showing microcrystalline to chalcedonic silica texture.

Despite the absence of taxonomically informative anatomy, these unassigned specimens are included because they represent the broader morphological and taphonomic spectrum of silicified wood in the assemblage (Fig. 5). Their macroscopic preservation and degree of rounding support interpretation of a fluvial transport history, consistent with that inferred for the identified *Cordaixylon* material.

Petrography and geochemistry

Polarizing microscope observations of thin sections confirmed that the cellular structure is infilled with quartz-group minerals, preserving the original anatomy and texture of the wood without major disruption. In addition to the predominant silica content, small amounts of iron oxides (Fe_xO_y) are present as pigments (Fig. 6G, H). Opaque minerals occasionally occur in the spaces between fossilized cells, while mica flakes are rare and appear only as isolated inclusions.

Across the thin sections, alternating light and dark parallel bands are clearly visible (Fig. 6B). Although they may superficially resemble growth rings, they are unrelated to the original plant anatomy. In some samples, the bands exhibit an irregular, undulating, or zigzag pattern, with their coloration determined by the distribution of iron compounds.

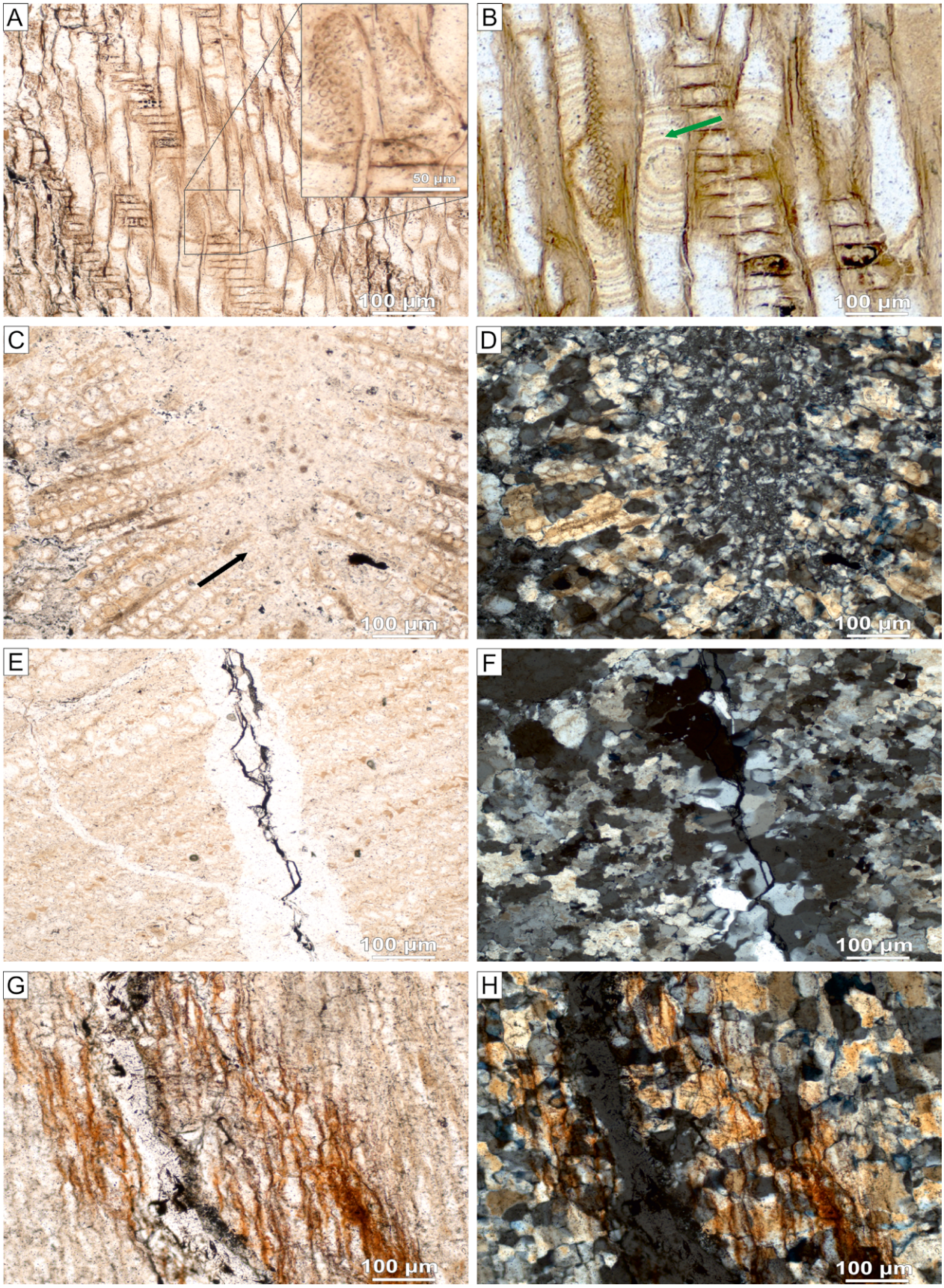

Fig. 6. Specimen 17KUD (A–D). **A.** Radial longitudinal section with distinct cross-field pitting, in PPL. **B**. Radial longitudinal section, showing distinct cross-field pitting and alternating light and dark parallel bands, resembling growth rings (green arrow), in PPL. **C**. Transverse section in PPL, illustrating microcrystalline quartz responsible for the petrification of tissues undergoing decomposition (black arrow). **D**. The same field of view in XPL. **E**, **F.** Specimen 10KUD; E – large idiomorphic megaquartz crystals commonly filling cracks within the tissue, in PPL; F – the same view shown in XPL. **G**, **H.** Specimen 13KUD; G – iron oxides (Fe_xO_y) visible as pigmentation despite the predominantly silica-rich composition, in PPL; H – the same view shown in XPL.

During fossilization, concentric precipitation of silica commonly occurred around cells or voids within the wood, producing secondary rings that reflect successive stages of mineral deposition (Fig. 6A). Cracks within the tissue were frequently filled by large idiomorphic megaquartz crystals (Fig. 6E, F).

In several thin sections, the silicified wood exhibits microstructures consistent with the so-called *Punctstein* texture (Fig. 6A–F), first described and illustrated by Cotta (1832) and recently recognized at several sites (Trümper *et al*., 2022). These features appear as fine, rounded or irregular silica-filled spots, typically less than 200 μm in diameter, scattered throughout the tissue matrix (Fig. 6). They are commonly located within or adjacent to cell walls and exhibit distinct optical contrast, relative to the surrounding matrix, under PPL. In this material, these structures are interpreted as an early stage of silica crystallization.

Further analytical techniques support the petrographic observations. The SEM-BSE image displays a nearly uniform gray appearance, with no discernible zoning within the quartz (Fig. 7A–D). This uniformity indicates that any trace elements substituting for quartz-lattice sites occur at concentrations too low to be detected, even at maximum contrast. The absence of detectable chemical heterogeneity suggests that silicification occurred under relatively stable, homogeneous conditions (see Supplementary Material S1). Such conditions would have promoted rapid stabilization of the cellular framework before significant biological or chemical degradation could take place, while remaining gentle enough to avoid introducing marked elemental variations. Consequently, the well-preserved cellular structure of the studied specimens faithfully reflects the original organization of the wood tissues.

Cathodoluminescence (CL) analyses provide additional, consistent evidence (Fig. 7E, F). The predominantly blue luminescence, observed in CL imaging is characteristic of microcrystalline quartz and displays a relatively homogeneous signal with no pronounced colour zoning. Cell outlines remain visible as slightly darker or lighter boundaries, confirming that mineralization preserved the original tissue morphology. Locally, small dark patches occur, most likely related to Fe-rich inclusions that dampen the CL signal. The overall homogeneity of the luminescence indicates monophase silicification, with only limited subsequent recrystallization. These observations support a model of early, rapid permineralization, mediated by the flow of silica-bearing fluids. Given the geological setting of the study area, however, silicification is unlikely to be attributed to a single controlling factor; a combination of diagenetic processes and hydrothermal fluid flow is probable. Interpretation is further complicated by the fact that the material was recovered from alluvial deposits, and the studied wood appears to have been redeposited within these sediments.

DISCUSSION

The silicified wood fragments from the Kudowa-Słone locality exhibit close anatomical and taphonomic affinities to fossil wood documented from the Czech sector of the ISB and other Late Palaeozoic basins of Central Europe (Mencl and Sakala, 2009; Trümper *et al*., 2020, 2022). The best-preserved specimens, assigned to *Cordaixylon* sp., display secondary xylem features, pit structures and cross-field characteristics that closely correspond to he cordaitalean woods described from the Žaltman Arkoses of the Odolov Formation. In those occurrences, the fossil wood from the Kudowa-Słone locality appears exclusively as disarticulated, barkless, and branchless fragments, confirming its allochthonous nature and reflecting mechanical fragmentation prior to its secondary deposition in late Quaternary deposits.

The distribution of cordaitalean wood within the Late Carboniferous strata of the southwestern ISB, particularly within the lower Jívka Member, strongly supports a provenance from Carboniferous outcrops, incised by the modern Metuje River, near Hronov. The anatomical structure recognized in the present specimens, which are well-preserved despite fluvial transport, indicates that silicification occurred early within their original Carboniferous host deposits. The combination of varying degrees of rounding of the wood debris and the coexistence of both diagnostic and non-diagnostic fragments suggests that even within the original Carboniferous deposits, the wood was not preserved *in situ* but had already been redeposited within fluvial sediments. This implies at least a two-stage reworking history, whereby the silicified trunks were first transported and incorporated in Carboniferous arkosic fluvial deposits and, following their burial and the post-Cretaceous uplift of the ISB basin margins, were subsequently exhumed, transported, and redeposited during Late Quaternary southward drainage.

Petrographic and geochemical analyses offer further insight into the silicification process and illuminate the diagenetic conditions under which the studied Carboniferous wood was mineralised. The uniform grey tone of quartz in BSE images, the absence of internal zoning or chemical banding, and the homogeneous blue CL emission all indicate essentially monophase silicification under relatively stable geochemical and thermal conditions. The preservation of anatomical structures indicates that silica infiltration occurred rapidly, before substantial biological degradation of the wood tissues. Concentric silica bands and *Punctstein* textures reflect fluctuations in silica saturation and crystal nucleation, but do not imply significant hydrothermal overprinting. These features are consistent with a model in which silicification was driven primarily by basin-scale diagenetic processes, although a contribution from silica-rich hydrothermal fluids cannot be excluded. In the Czech sector of the ISB, silicification has been directly linked to volcanic and tectonic activity that facilitated the mobilisation of silica in pore waters, and similar conditions may have prevailed in the Polish part of the basin. Late Carboniferous–Early Permian sill-like intrusions are documented across both the western and eastern limbs of the ISB, providing a plausible magmatic heat source that could have enhanced fluid circulation and promoted silica precipitation (Awdankiewicz, 1999a, b). The comparison of the Kudowa-Słone specimens with silicified wood from the Nowa Ruda region (Dziedzic, 1959) further highlights the consistency of the taphonomic and mineralisation patterns across the basin. Although

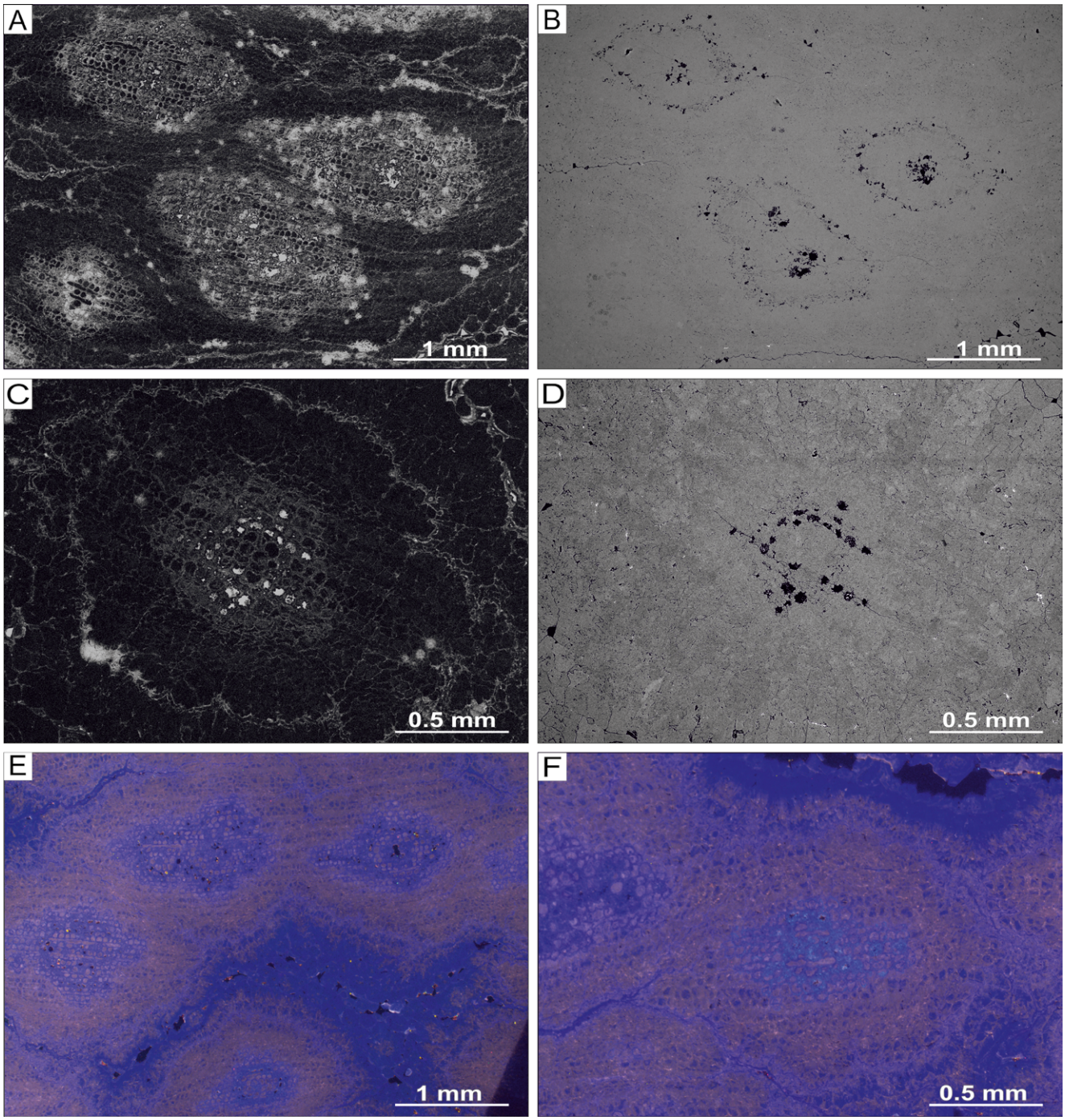

Fig. 7. Selected images from the SEM microscope and CL module. Specimen 13KUD. **A**–**D.** The general view of the transverse section with the arrangement of plant cells and visible Punctstein (pointstone) texture, shown in SEM-BSE images. **E–F.** The same section under CL imaging, highlighting mineral luminescence and tissue structure.

Quaternary transport may have induced microfracturing and minor recrystallisation along fracture networks within the wood, the primary mineralogical fabric of the wood remains largely intact. The Kudowa-Słone material thus exemplifies the long-term resistance of silicified wood.

Sedimentological data from the Kudowa-Słone locality provide a well-constrained framework for reconstructing the reworking processes and transport mechanisms of the silicified wood debris. The gravel-dominated succession records deposition in a high-energy braided or transitional mixed-load perennial river, characterised by bedload-dominated transport, relatively rapid sediment aggradation, and recurrent high-magnitude (?) flood events. Clast imbrication, the orientation of cross-bedding, and the measured axes of fluvial channels collectively document a southward palaeoflow, with secondary dispersal toward the SE and SW that corresponds closely to the present-day course of the Metuje River. The petrographic composition of the gravels further constrains the directions of clastic material supply. The dominant contribution from Upper Cretaceous sandstones and siliceous mudstones reflects input from the north, sourced from the western part of the

Intra-Sudetic Basin within the catchment of the Metuje River and its tributary, the Dřevíč Stream, whereas granitoids, quartz, and metamorphic rock clasts were derived from neighbouring massifs to the south and east, transported in part by the Klikawa Stream. In addition, Lower Permian conglomerates and sandstones were derived from the Brzozowie Graben area. Taken together, these sedimentological and petrographic data strongly support the interpretation that the silicified wood fragments were eroded during Late Quaternary incision of the Metuje River and the Dřevíč Stream into Carboniferous strata, and were subsequently transported southward, likely over a distance of 7–10 km, predominantly as coarse bedload during peak-flow events.

CONCLUSION

The silicified wood fragments, recovered in this study from the Kudowa-Słone locality, are assigned to the genus *Cordaixylon*, representing cordaitalean trees that formed an essential component of Late Palaeozoic forest ecosystems in the ISB and other late- and post- Variscan continental basins across Central Europe. Despite being preserved as disarticulated, barkless and branchless fragments redeposited within unconsolidated Late Quaternary alluvial deposits, the specimens retain exceptionally well-preserved secondary xylem anatomy. This combination of high anatomical fidelity and pronounced physical damage indicates that the wood is allochthonous and has undergone a complex, multistage taphonomic history. Sedimentological and palaeobotanical evidence suggest that the material was derived from the Carboniferous sedimentary successions and had already experienced at least two phases of fluvial redeposition: first in Pennsylvanian arkosic channel deposits, and later in Late Quaternary fluvial sediments.

Integrating sedimentological data, clast petrography and regional geological constraints, the authors infer that the most plausible source area for the silicified trunks lies in the southwestern, Czech part of the ISB, specifically within the Jívka Member of the Odolov Formation. In this area, cordaitalean wood is abundant in arkosic fluvial strata, incised by the entrenched valleys of the present-day Metuje River and its tributary, the Dřevíč Stream, near Hronov. During Late Quaternary incision, erosion of these Carboniferous strata entrained the silicified trunks as bedload and transported them likely during high-magnitude floods, before their deposition in the gravelly terrace sediments at Kudowa-Słone. This study demonstrates that early silicification, followed by later fluvial reworking, can decouple fossil wood from its original stratigraphic context, while preserving a robust record of both Palaeozoic vegetation and Quaternary fluvial dynamics.

Acknowledgments

We sincerely thank Bogusław Przybylski (PGI-NRI, Wrocław) for his invaluable support during the fieldwork and for his assistance with the analysis of Quaternary sediments. We are also grateful to Ewa Krzemińska and Dominik Gurba (PGI-NRI, Warsaw) for their collaboration and for providing technical support with the SEM and CL imaging. We would also like to thank Magdalena Furca (PGI-NGI, Wrocław) for her help in photographing the specimens. Special thanks to Aleksander Gomółka for providing access to the studied exposure. We also extend our gratitude to Václav Mencl (Institute of Geology of the Czech Academy of Sciences, Prague, Czech Republic) and Grzegorz Pacyna (Institute of Geological Sciences, Jagiellonian University, Kraków, Poland) for their valuable reviews and insightful comments, which significantly improved this manuscript. We further thank Paweł Filipiak (Institute of Earth Sciences, University of Silesia in Katowice, Poland) for his support during the editorial process. This research was carried out as a result of Statutory Project No. 61.2611.2500.00 of the Polish Geological Institute-National Research Institute. The geological mapping survey described in this paper was funded by the Ministry of the Climate and Environment of Poland from the sources of the National Fund for Environment Protection and Water Management (project no. 22.1509.2102.00.1: „Wykonanie czterech arkuszy Szczegółowej Mapy Geologicznej Sudetów w skali 1:25 000: Radków i Pasterska Góra, Kudowa Zdrój i Brzozowice, Wambierzyce oraz Polanica Zdrój").

REFERENCES

Akahane, H., Furuno, T., Miyajima, H., Yoshikawa, T. & Yamamoto, S., 2004. Rapid wood silicification in hot spring water: an explanation of silicification of wood during the Earth's history. *Sedimentary Geology*, 169: 219–228.

Allen, J. R. L., 1982. *Sedimentary Structures: Their Character and Physical Basis. Volume 1. Developments in Sedimentology.* Elsevier, Amsterdam, 593 pp.

Augustyniak, K. & Grocholski, A., 1968. Geological structure and outline of the development of the Intra-Sudetic Depression. *Biuletyn Instytutu Geologicznego*, 17: 87–111.

Awdankiewicz, M., 1999a. Volcanism in a late Variscan intramontane trough: Carboniferous and Permian volcanic centres of the Intra-Sudetic Basin, SW Poland. *Geologia Sudetica*, 32: 13–47.

Awdankiewicz, M., 1999b. Volcanism in a late Variscan intramontane trough: the petrology and geochemistry of the Carboniferous and Permian volcanic rocks of the Intra-Sudetic Basin, SW Poland. *Geologia Sudetica*, 32: 83–111.

Brenna, A., Martini, I., Menapace, L., Surian, N., Ventra, D. & Ghinassi, M., 2024. Imbrication fabric as a diagnostic feature for the genetic classification of gravels deposited by fluid-gravity versus sediment-gravity subaerial flows. *Earth Surface Processes and Landforms*, 49: 4088–4098.

Bridge, J. S., 2003. *Rivers and Floodplains: Forms, Processes, and Sedimentary Record.* Wiley-Blackwell, Oxford, 487 pp.

Brzyski, B., 1969. Tissue structures of fossilized remains of Carboniferous flora (Namur A) from the Upper Silesian Coal Basin. *Acta Palaeobotanica*, 10: 3–98. [In Polish, with English summary.]

Brzyski, B., 2001. Flora szczątków skamieniałych z osadów karbonu Polski (z zachowaniem budowy anatomicznej). In: Pajchlowa, M. (ed.), *Budowa geologiczna Polski. T. III, Atlas skamieniałości przewodnich i charakterystycznych. Część 1c, z. 2, Młodszy paleozoik, karbon, flora*. Państwowy Instytut Geologiczny i Ministerstwo Środowiska, Warszawa, pp. 845–855. [In Polish.]

Cartigny, M. J. B., Ventra, D., Postma, G. & Van den Berg, J. H., 2014. Morphodynamics and sedimentary structures of bedforms under supercritical-flow conditions: New insights from flume experiments. *Sedimentology*, 61: 712–748.

Cháb, J., Breiter, K., Fatka, O., Hladil, J., Kalvoda, J., Šimůnek, Z., Štorch, P., Vašíček, Z., Zajíc, J. & Zapletal, J., 2010. *Outline of the Geology of the Bohemian Massif: The Basement Rocks and Their Carboniferous and Permian Cover.* Czech Geological Survey, Prague, 295 pp.

Cleal, C. J. & Thomas, B. A., 2005. Palaeozoic tropical rainforests and their effect on global climates: is the past the key to the present? *Geobiology*, 3: 13–31.

Collinson, J. D., 1996. Alluvial sediments. In: Reading, H. G. (ed.), *Sedimentary Environments: Processes, Facies and Stratigraphy*. Blackwell Publishing, Oxford, pp. 37–82.

Cotta, C. B., 1832. Anhang vulgo Punctstein. In: *Die Dendrolithen in Beziehung auf ihren inneren Bau.* Arnoldische Buchhandlung, Dresden und Leipzig, pp. 54–56.

Cymerman, Z., 1997. Structure, kinematics, and an evolution of the Orlica-Śnieżnik Dome, Sudetes. *Prace Państwowego Instytutu Geologicznego*, 156: 1–120.

Cymerman, Z., 2019a. *Szczegółowa Mapa Geologiczna Polski 1:50 000, arkusz 899 – Kudowa Zdrój.* Państwowy Instytut Geologiczny – Państwowy Instytut Badawczy, Warszawa. [In Polish.]

Cymerman, Z., 2019b. *Objaśnienia do Szczegółowej Mapy Geologicznej Polski w skali 1:50 000. Arkusz Kudowa Zdrój (899) i Duszniki Zdrój (900).* Państwowy Instytut Geologiczny – Państwowy Instytut Badawczy, Warszawa, 50 pp. [In Polish.]

DiMichele, W. A., 2014. Wetland-dryland vegetational dynamics in the Pennsylvanian Ice Age tropics. *International Journal of Plant Sciences*, 175: 123–164.

Dziedzic, K., 1959. On a new occurrence of silicified trunks in the Upper Carboniferous of the Intrasudetic Basin. *Rocznik Polskiego Towarzystwa Geologicznego*, 28: 427–432. [In Polish, with English summary.]

Dziedzic, K. & Teisseyre, A. K., 1990. The Hercynian molasse and younger deposits in the Intra-Sudetic Depression, SW Poland. *Neues Jahrbuch für Geologie und Paläontologie*, 179: 285–305.

Farr, T. G., Rosen, P. A., Caro, E., Crippen, R., Duren, R., Hensley, S., Kobrick, M., Paller, M., Rodriguez, E., Roth, L., Seal, D., Shaffer, S., Shimada, J., Umland, J., Werner, M., Oskin, M., Burbank, D. & Alsdorf, D., 2007. The Shuttle Radar Topography Mission. *Reviews of Geophysics*, 45: RG2004.

Fielding, C. R., 2006. Upper flow regime sheets, lenses and scour fills: Extending the range of architectural elements for fluvial sediment bodies. *Sedimentary Geology*, 190: 227–240.

Florjan, S., 2012. The first discovery in Poland of an isolated mineralized core of a Carboniferous cordaite shoot. *Przegląd Geologiczny*, 60: 322–324. [In Polish, with English abstract.]

Gierwielaniec, J., 1955. *Szczegółowa Mapa Geologiczna Sudetów. Arkusz Kudowa Zdrój 1:25 000.* Wydawnictwa Geologiczne, Warszawa. [In Polish.]

Gierwielaniec, J., 1965. Geological structure of the vicinity of Kudowa-Zdrój. *Biuletyn Instytutu Geologicznego*, 185: 23–90. [In Polish, with English summary.]

Głuszyński, A. & Aleksandrowski, P., 2022. Late Cretaceous–Early Palaeogene inversion-related tectonic structures at the NE margin of the Bohemian Massif (SW Poland and northern Czechia). *Solid Earth*, 13: 1219–1242.

Grand'Eury, F. C., 1877. La flore carbonifére du Département de la Loire et du centre de la France, étudiée aux trois points de vue botanique, stratigraphique et géognostique. *Mémoires présentés par divers savants l'Académie des Sciences de l'Institut de France*, 24: 1–624.

Harms, J. C., Southard, J. B., Spearing, D. R. & Walker, R. G., 1975. *Depositional Environments as Interpreted from Primary Sedimentary Structures and Stratification Sequences.* In: Harms, J. C, Southard, J. B., Spearing, D. R. & Walker, R. G. (eds), *SEPM Short Course Notes*. SEPM Society for Sedimentary Geology, Dallas, pp. 1–20.

Kowalski, A., 2020. Triassic palaeogeography of NE Bohemian Massif based on sedimentological record in the Wleń Graben and the Krzeszów Brachysyncline (SW Poland). *Annales Societatis Geologorum Poloniae*, 90: 125–148.

Kowalski, A., 2021. Late Cretaceous palaeogeography of NE Bohemian Massif: diachronous sedimentary successions in the Wleń Graben and Krzeszów Brachysyncline (SW Poland). *Annales Societatis Geologorum Poloniae*, 91: 1–36.

Kowalski, A., Przybylski, B., Kozdrój, W. & Bubel, P., 2024a. *Szczegółowa Mapa Geologiczna Sudetów w skali 1:25 000. Arkusz Kudowa Zdrój (899B) i Brzozowice (899D).* Państwowy Instytut Geologiczny – Państwowy Instytut Badawczy, Warszawa. [In Polish.]

Kowalski, A., Przybylski, B., Kozdrój, W. & Bubel, P., 2024b. *Objaśnienia do Szczegółowej Mapy Geologicznej Sudetów w skali 1:25 000. Arkusz Kudowa Zdrój (899B) i Brzozowice (899D)*. Państwowy Instytut Geologiczny – Państwowy Instytut Badawczy, Warszawa, 63 pp. [In Polish.]

Kurowski, L., 1998. Fluvial sedimentology of the Biały Kamień Formation (Upper Carboniferous, Sudetes, Poland). *Geologia Sudetica*, 31: 69–77.

Lang, J. & Winsemann, J., 2013. Lateral and vertical facies relationships of bedforms deposited by aggrading supercritical flows: From cyclic steps to humpback dunes. *Sedimentary Geology*, 296: 36–54.

Madej, S., 2023. Skamieniałe drewno – geneza i przykłady okazów z wybranych lokalizacji w Polsce i na świecie. In: Pietranik A., Trojanowska-Olichwer A. (eds), *Zatrzymane w Czasie – Skamieniałości i Bursztyny.* XXIV Lwóweckie Lato Agatowe, Lwówecki Ośrodek Kultury, Lwówek Śląski, pp. 11–19. [In Polish.]

Mastalerz, K., 1990. Lacustrine successions in fault-bounded basins: 1. Upper Anthracosia Shale (Lower Permian) of the North Sudetic Basin, SW Poland. *Annales Societatis Geologorum Poloniae*, 60: 75–106.

Mastalerz, K., 1996. Fluvial sedimentation of the coal-bearing Žacler Formation (Westphalian) in the Wałbrzych Basin, SW Poland. *Acta Universitatis Wratislaviensis, Prace Geologiczno-Mineralogiczne*, *Z badań karbonu i permu w Sudetach*, 52: 21–85. [In Polish, with English summary.]

Matysová, P., Leichmann, J., Grygar, T. & Rössler, R., 2008. Cathodoluminescence of silicified trunks from the Permo–Carboniferous basins in eastern Bohemia, Czech Republic. *European Journal of Mineralogy*, 20: 217–231.

Mencl, V. M., Bureš, J. & Sakala, J., 2013. Summary of occurrence and taxonomy of silicified agathoxylon-type of wood in Late Paleozoic basins of the Czech Republic. *Folia Musei rerum*

naturalium Bohemiae occidentalis Geologica et Paleobiologica, 47: 14–26.

Mencl, V. M. & Sakala, J., 2009. Silicified wood from the Czech part of the Intra-Sudetic Basin (Late Pennsylvanian, Bohemian Massif, Czech Republic): systematics, silicification and palaeoenvironment. *Neues Jahrbuch für Geologie und Paläontologie – Abhandlungen*, 252: 269–288.

Miall, A. D., 1977a. A review of the braided-river depositional environment. *Earth-Science Reviews*, 13: 1–62.

Miall, A. D., 1977b. Lithofacies types and vertical profile models in braided river deposits: A summary. In: Miall, A. D (ed.), *Fluvial Sedimentology.* Geological Survey of Canada, Calgary, pp. 597–604.

Miall, A. D., 1996. *The Geology of Fluvial Deposits. Sedimentary Facies, Basin Analysis, and Petroleum Geology.* Springer, Berlin, 582 pp.

Miall, A. D., 2014. *Fluvial Depositional Systems.* Springer, Cham, 316 pp.

Mroczkowski, J. & Mader, D., 1985. Sandy inland braidplain deposition with local aeolian sedimentation in the lower and middle parts of the Buntsandstein and sandy coastal braidplain deposition in the topmost Zechstein in the Sudetes (Lower Silesia, Poland). In: Mader D. (ed.), *Aspects of Fluvial Sedimentation in the Lower Triassic Buntsandstein of Europe.* Springer-Verlag, Berlin, pp. 165–195.

Mustoe, G., 2015. Late Tertiary petrified wood from Nevada, USA: Evidence of multiple silicification pathways. *Geosciences*, 5: 286–309.

Mustoe, G. E., 2023. Silicification of wood: An overview. *Minerals*, 13: 206.

Nemec, W., 1984. Wałbrzych Beds (Lower Namurian, Wałbrzych Coal Measures): Analysis of alluvial sedimentation in a coal basin. *Geologia Sudetica*, 19: 7–73. [In Polish, with English summary.]

Nemec, W., Porębski, S. J. & Teisseyre, A. K., 1982. Explanatory notes to the lithotectonic molasse profile of the Intra-Sudetic Basin, Polish part (Sudety Mts., Carboniferous–Permian). In: Schwab, G. (ed.), *Tectonic Regime of Molasse Epochs.* Veröffentlichungen des Zentralinstituts für Physik der Erde, Potsdam, pp. 267–278.

Noll, R., 2012. Anatomische Beobachtungen am Sekundärxylem permischer Koniferen- und Cordaitenhölzer der Donnersberg-Formation. *Veröffentlichungen des Museums für Naturkunde Chemnitz*, 35: 29–38.

Nováková, L., 2014. Evolution of paleostress fields and brittle deformation in the Hronov-Poříčí Fault Zone, Bohemian Massif. *Studia Geophysica et Geodaetica*, 58: 269–288.

Nowak, G. J. & Górecka-Nowak, A., 1999. Peat-forming environments of Westphalian A coal seams from the Lower Silesian Coal Basin of SW Poland based on petrographic and palynologic data. *International Journal of Coal Geology*, 40: 327–351.

Opluštil, S., Eble, C., Šimůnek, Z. & Drábková, J., 2024. Paleoenvironment and vegetational history of a Middle Pennsylvanian intramontane peat swamp: an example from the Lower Radnice Coal, Kladno coalfield (Czech Republic). *International Journal of Earth Sciences*, 113: 1949–1975.

Opluštil, S. & Pešek, J., 1998. Stratigraphy, palaeoclimatology and palaeogeography of the Late Palaeozoic continental deposits in the Czech Republic. *Geodiversitas*, 20: 597–620.

Opluštil, S., Schmitz, M., Kachlík, V. & Štamberg, S., 2016. Re-assessment of lithostratigraphy, biostratigraphy, and volcanic activity of the Late Paleozoic Intra-Sudetic, Krkonoše-Piedmont and Mnichovo Hradiště basins (Czech Republic) based on new U-Pb CA-ID-TIMS ages. *Bulletin of Geosciences*, 91: 399–432.

Pešek, J., Holub, V., Jaroš, J., Malý, L., Martinek, K., Prouza, V., Spudil, J. & Tásler, R., 2001. *Geologie a ložiska svrchnopaleozoických limnických pánví České republiky.* Český Geologický Ústav, Praha, 254 pp. [In Czech.]

Prouza, V., Coubal, M. & Adamovic, J., 2015. Specifika architektury hronovsko-poříčského zlomu. *Zprávy o Geologickém Výzkumu v Roce 2014*, 2014: 13–18. [In Czech.]

Rößler, R., Philippe, M., van Konijnenburg-van Cittert, J. H. A., McLoughlin, S., Sakala, J., Zijlstra, G., Annamraju, R., Ash, S., Baas, P., Bamford, M., Bateman, R., Booi, M., Boonchai, N., Brea, M., Crisafulli, A., Decombeix, A.-L., Dolezych, M., Dutra, T., Esteban, L. G., Falaschi, P., Falcon-Lang, H., Feng, Z., Gnaedinger, S., Guerra Sommer, M., Harland, M., Herbst, R., Hilton, J., Iamandei, E., Iamandei, S., Jiang, H.-H., Jiang, Z., Kim, K., Kunzmann, L., Kurzawe, F., Merlotti, S., Meyer-Berthaud, B., Naugolnykh, S., Nishida, H., Oh, C., Orlova, O., de Palacios, P., Pole, M., Poole, I., Pujana, R., Ryberg, P., Savidge, R., Schultka, S., Süß, H., Taylor, E., Terada, K., Thévenard, F., Torres, T., Vera, E., Wheeler, E., Yang, X.-j., Zheng, S. & Zhang, W., 2014. Which name(s) should be used for Araucaria-like fossil wood? Results of a poll. *Taxon*, 63: 177–184.

Rößler, R., Trümper, S., Noll, R., Hellwig, A. & Niemirowska, S., 2021. Wood shrinkage during fossilisation and its significance for studying deep-time lignophytes. *Review of Palaeobotany and Palynology*, 292: 104455.

Sawicki, L., 1995. *Geological Map of Lower Silesia with Adjacent Czech and German Territories (without Quaternary Deposits).* Państwowy Instytut Geologiczny, Warszawa.

Schneider, J. W., Lucas, S. G., Scholze, F., Voigt, S., Marchetti, L., Klein, H., Opluštil, S., Wernerburg, R., Golubev, V. K., Barrick, J. E., Nemyrovska, T., Ronchi, A., Day, M. O., Silantiev, V. V., Rößler, R., Saber, H., Linnemann, U., Zharinova, V. & Shu-Zhong, S., 2020. Late Paleozoic–early Mesozoic continental biostratigraphy – Links to the Standard Global Chronostratigraphic Scale. *Palaeoworld*, 29: 186–238.

Schöpfer, K., Nádaskay, R. & Martínek, K., 2022. Evaluation of climatic and tectonic imprints in fluvial successions of an Early Permian depositional system (Asselian Vrchlabí Formation, Krkonoše Piedmont Basin, Czech Republic). *Journal of Sedimentary Research*, 92: 275–303.

Slootman, A. & Cartigny, M. J. B., 2020. Cyclic steps: Review and aggradation-based classification. *Earth-Science Reviews*, 201: 102949.

Sternberg, K. M., 1820. *Versuch einer geognostisch-botanischen Darstellung der Flora der Vorwelt.* Fleischer, Leipzig, 824 pp.

Tásler, R., Čadková, Z., Dvořák, J., Fediuk, F., Chaloupský, J., Jetel, J., Kaiserová-Kalibová, M., Prouza, V., Schovánková-Hrdličková, D., Středa, J., Střída, M. & Šetlík, J., 1979. *Geology of the Bohemian Part of the Intra-Sudetic Basin*. Academia, Praha, 292 pp. [In Czech, with English summary.]

Teisseyre, A. K., 1991. River classification in the light of analysis of the fluvial system and hydraulic geometry. *Prace Geologiczno-Mineralogiczne*, 22: 1–210. [In Polish, with English summary.]

Trümper, S., Gaitzsch, B., Schneider, J. W., Ehling, B., Kleeberg, R. & Rößler, R., 2020. Late Palaeozoic red beds elucidate fluvial architectures preserving large woody debris in the seasonal tropics of central Pangaea. *Sedimentology*, 67: 1973–2012.

Trümper, S., Mencl, V., Opluštil, S., Niemirowska, S. & Rößler, R., 2022. Large woody debris accumulations in the late Pennsylvanian tropics – evolutionary signal or tectono-climatic archive? *Palaios,* 37: 251–291.

Trümper, S., Rößler, R. & Götze, J., 2018. Deciphering silicification pathways of fossil forests: Case studies from the Late Paleozoic of Central Europe. *Minerals*, 8: 432.

Turnau, E., Żelaźniewicz, A. & Franke, W., 2002. Middle to early late Viséan onset of late orogenic sedimentation in the Intra-Sudetic Basin, West Sudetes: miospore evidence and tectonic implication. *Geologia Sudetica*, 34: 9–16.

Weckwerth, P., Kalińska, E., Wysota, W., Krawiec, A., Alexanderson, H. & Chabowski, M., 2024. Evolutionary model for glacial lake-outburst fans at the ice-sheet front. *Geomorphology*, 453: 109125.

Wojewoda, J., 1997. Upper Cretaceous littoral-to-shelf succession in the Intrasudetic Basin and Nysa Trough. *Obszary Źródłowe – Zapis w Osadach*, 1: 81–96.

Wojewoda, J., 2009. Žďarky-Pstrążna Dome: a strike-slip fault-related structure at the eastern termination of the Poříčí-Hronov Fault Zone (Sudetes). *Acta Geodynamica et Geomaterialia*, 6: 273–290.

Wojewoda, J. & Burliga, S., 2008. Clastic dikes and seismotectonic breccia in Permian deposits of the Nachod Basin (Middle Sudetes). *Przegląd Geologiczny*, 56: 857–862. [In Polish, with English abstract.]

Wojewoda, J. & Mastalerz, K., 1989. Climate evolution, allo- and autocyclicity of sedimentation: an example from the Permo–Carboniferous continental deposits of the Sudetes, SW Poland. *Przegląd Geologiczny*, 37: 173–180. [In Polish, with English summary.]

Żelaźniewicz, A., 1977a. Granitoids of the Kudowa-Olešnice Massif (Sudetes). *Geologia Sudetica*, 12: 137–162. [In Polish, with English summary.]

Żelaźniewicz, A., 1977b. Tectonic and metamorphic events in the Polish part of the Orlickie Mts. *Geologia Sudetica*, 11: 101–177.